Materials Science

DOI: 10.1002/anie.201106767

Self-Assembled Gelators for Organic Electronics

*Sukumaran Santhosh Babu, Seelam Prasanthkumar, and Ayyappanpillai Ajayaghosh**

charge transfer · gels · molecular devices · self-assembly · solar cells

Nature excels at engineering materials by using the principles of chemical synthesis and molecular self-assembly with the help of noncovalent forces. Learning from these phenomena, scientists have been able to create a variety of self-assembled artificial materials of different size, shapes, and properties for wide ranging applications. An area of great interest in this regard is solvent-assisted gel formation with functional organic molecules, thus leading to one-dimensional fibers. Such fibers have improved electronic properties and are potential soft materials for organic electronic devices, particularly in bulk heterojunction solar cells. Described herein is how molecular self-assembly, which was originally proposed as a simple laboratory curiosity, has helped the evolution of a variety of soft functional materials useful for advanced electronic devices such as organic field-effect transistors and organic solar cells. Highlights on some of the recent developments are discussed.

1. Introduction

Nature has the unparalleled ability to create a variety of self-assembled soft materials. These materials function elegantly and efficiently within soft tissues under aqueous conditions for years without failure. In contrast, man-made soft materials of molecular assemblies cannot, in most of the cases, be directly applied to useful applications, particularly in electronic devices. Therefore, inorganic materials have been dominating in the fabrication of the so-called hard electronic devices. However, the quest for improved performance and miniaturization of devices is driving technologies to attain newer heights with organic-molecule-based functional materials. These soft electronic materials have given birth to the so-called organic/plastic electronics. In parallel, the idea of molecular or supramolecular electronics has been proposed and are still at the conceptual level. For these technologies to develop, it is necessary to design stable, shape-persistent materials at the nanometer scale wherein the individual molecular building blocks are self-organized. Sensible design and logical selection of molecular components and interaction modes are the key points in achieving the design of such materials.[1,2]

Over the years, organogelation has emerged as an excellent strategy for crafting supramolecular assemblies with tunable properties that underpin the role of a solvent-directed approach to the design of functional materials.[3–11] Particularly, the last decade has witnessed important developments in the field of molecular gels and soft matter with electronic properties because of the ability to convert information at the molecular level into information at the nanoscopic and macroscopic levels in a spectacular way.[7–9] Obviously, π-conjugated molecules are the molecules of choice because of their tunable optoelectronic properties. A variety of π systems have been used in the preparation of organogels comprising supramolecular structures of different sizes, shapes, and properties. Thus, a number of organogels with electronic conductivity and charge-carrier mobility have been reported and may find applications in organic field-effect transistors (OFETs) and organic solar cells (OSCs). These developments have strengthened the potential of gel chemistry as a tool to create optimized functional assemblies. The technological or practical relevance of this concept is the tunable sizes, shapes, and optoelectronic properties of molecular gelators and the capability of the gel matrix to accommodate various components to achieve efficient charge transport properties. Even though the initial results are promising, the real application of organogelators in electronic devices is still at a premature stage and no breakthrough has been achieved so far. The total

[*] Dr. S. S. Babu, S. Prasanthkumar, Dr. A. Ajayaghosh
Photosciences and Photonics Group, Chemical Sciences and Technologies Division, National Institute for Interdisciplinary Science and Technology (NIIST), CSIR, Trivandrum (India)
E-mail: ajayaghosh62@gmail.com
Homepage: http://w3rrlt.csir.res.in/photo/people/draajayaghosh/Homepage.html

number of research articles with respect to the application of gels in the development of energy efficient devices is limited. Therefore, intense research and in-depth studies are needed to optimize the performance of gel-based electronic materials.

In this Minireview we highlight the recent developments in the field of self-assembled soft materials with electronic functions, and the role of gel chemistry as well as its future prospects in the area of organic electronics, particularly organic photovoltaics. We describe how the conceptually novel idea of molecular self-assembly, which was originally proposed as a simple laboratory curiosity, has over the years evolved into a technologically relevant topic dealing with advanced materials for a variety of electronic devices. To sensitize the reader with respect to the application potential, we first discuss the recent involvement of self-assemblies and gels in OSCs and OFETs and then move on to recent examples of electronically relevant gelators.

Sukumaran Santhosh Babu received his Ph.D. in 2009 from the National Institute for Interdisciplinary Science and Technology in India under the supervision of Dr. A. Ajayaghosh. He is currently a postdoctoral fellow with Dr. Takashi Nakanishi in Japan after completing one year at the MPI-NIMS International joint laboratory in Germany led by Prof. Helmuth Möhwald and Dr. Takashi Nakanishi. His research interests include self-assembly, photophysical properties, and applications of supramolecular functional assemblies.

Seelam Prasanthkumar obtained an M.Sc. (Chemistry) from the Hyderabad Central University, Hyderabad, Andhrapradesh, India in 2005. He has been working towards his Ph.D. since 2006 with Dr. A. Ajayaghosh. His research is focused on conducting organogels: design, synthesis, and self-assembly of oligo(thienylenevinylene)-derived molecular wires.

Ayyappanpillai Ajayaghosh is a CSIR outstanding scientist at the National Institute for Interdisciplinary Science and Technology in Trivandrum, Dean of Chemical Sciences at the Academy of Scientific and Innovative Research in New Delhi, and a fellow of the Indian Academy of Sciences in Bangalore. His research interests include functional organic and macromolecular materials, functional dyes and fluorophores, molecular self-assemblies and nanostructures, organogels, light-harvesting assemblies, and molecular probes.

2. Organogels in Photovoltaics

The last decade has witnessed a surge of activities in solar energy conversion using organic photovoltaic devices.[12,13] The advantages of OSCs include the availability of a large number of chemical structures, ease of processing, mechanical flexibility, and low cost.[14] An important requirement for an OSC device is the nanometer-scale, supramolecular ordering of the donor (D) and the acceptor (A) to control the bulk separation of photoinduced excitons through the nanophase separation resulting in bulk heterojunctions (BHJ) with high light-conversion efficiency.[15] As an initial step, low-molecular-weight gelators have been used in dye-sensitized solar cells (DSSC) as a quasisolid gelled electrolyte to carry the volatile organic solvent intact inside the solar cell, thus leading to production advantages and better performance of the device.[16–18]

Among thin-film devices, BHJ SCs of regioregular poly(3-hexylthiophene) (P3HT; **1**; Scheme 1) and [6,6]-phenyl-C_{61}-butyric acid methyl ester (PCBM) have been reported as one of the extensively studied systems.[19] Numerous studies such as thermal or solvent annealing procedures, and the effects of regioregularities and molecular weights of donors have been carried out to improve the efficiency and end-use performance of this donor–acceptor (D–A) system.[20] Recently, the effect of time- or concentration-dependent gelation and optical changes of **1** on the solar cell performance was studied by Huang and co-workers.[21] The performance of **1**/PCBM BHJ SCs indicated that devices having photoactive layers that were spin-coated using *o*-xylene solutions and a shorter aging time showed a gradual increase in short-circuit current density (J_{sc}). As compared to the samples aged for longer time, a better performance was exhibited by the device prepared after 2 hours of aging and showed a J_{sc} value of 12.57 mA cm^{-2}, open-circuit photovoltage (V_{oc}) of 0.59 V, fill factor (FF) of 0.51, and a reasonably high power conversion efficiency (PCE) of 3.78%.

The molecular weight (M_W) of the gelators has a significant influence on the gelation behavior, as demonstrated in the case of different batches of the polythiophene **1**, and in turn this behavior is reflected in the device performance. A solution of a low-molecular-weight polymer ($M_W = 26200$, $M_n = 13000$ g mol^{-1}) showed no sign of gelation, whereas solutions of an average-molecular-weight polymer ($M_W = 72800$, $M_n = 34400$ g mol^{-1}) turned into gel within a few minutes, and the gelation of high-molecular-weight polymer ($M_W = 153800$, $M_n = 62500$ g mol^{-1}) was spontaneous (Figure 1a).[22] A correlation between solar cell performance and molecular weight revealed that a significant enhancement in the solar cell performance could be obtained with a mixture of 80 wt% of low-molecular-weight and 20 wt% of high-molecular-weight polymers. Because of the better phase separation and reduced recombination between polymer **2** and PCBM, photovoltaic devices fabricated using fibrous aggregates of the ultrasonicated polymer gel containing PCBM exhibited enhanced performance.[23] Interestingly, the polymeric gel fibers exhibited a higher hole mobility and at the same time increased J_{sc} values without change in the V_{oc} values. Hence the fabrication of solar cells using a preassembled polymer gel suspension is a promising tool for increasing the overall power conversion efficiency without decrease in the V_{oc} value. In another report, spray-coated thin films of nanoporous, submicron gel particles of **1** dispersed in

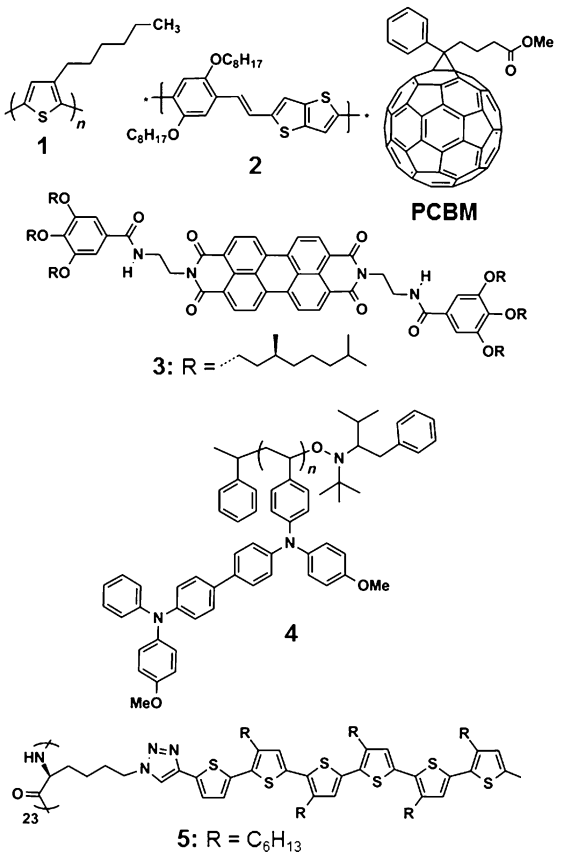

Scheme 1. Chemical structure of compounds **1**–**5**.[21–26]

surfactant-containing water has been used as solution-processable inks in solar cells.[24] Solar cells fabricated in combination with PCBM exhibited a PCE of 0.18% (J_{sc} = 1.2 mA cm^{-2}, V_{oc} = 0.42 V and FF = 0.36). This work highlights the use of novel functional coatings in organic electronics and can be extended to a variety of π gels.

Hydrogen-bond directed self-assembly of the low-molecular-weight, n-type perylene bisimide organogelator **3** (Scheme 1) in the presence of an amorphous p-type poly(vinyl-dimethoxytetraphenylbenzidine) polymer **4** has been used to generate nanostructures with large-area D–A interfaces suitable for an ideal supramolecular p–n heterojunction (Figure 1b).[25] The solar cell device of **3** and **4** (3:1) showed maximum efficiency with a J_{sc} value of 0.28 mA cm^{-2}, V_{oc} value of 390 mV, FF of 38%, and a PCE of 0.041% (Figure 1b). The better performance of this system could be due to the absence of large-scale macrophase separation of the donor and the acceptor molecules resulting in morphological stability. In addition, the BHJ devices comprised of **5** and PCBM (1:2) showed enhanced efficiency and short-circuit current. This enhancement could be attributed to the significantly high J_{sc} value obtained through the helical arrangement of chromophores, which resulted in favorable charge transport domains.[26]

A self-sorting approach to organogels of D–A systems is useful to the design of heterojunction organic semiconductors. For example, the two-component gel of thiophene **6** and perylenebisimide **7** (Scheme 2), composed of entangled fibrous aggregates is useful for the fabrication of photovoltaic devices.[27] The fiber crossing points are equivalent to p-n heterojunctions (Figure 2a). Upon visible-light irradiation, anodic photocurrent was generated from the cast films. In

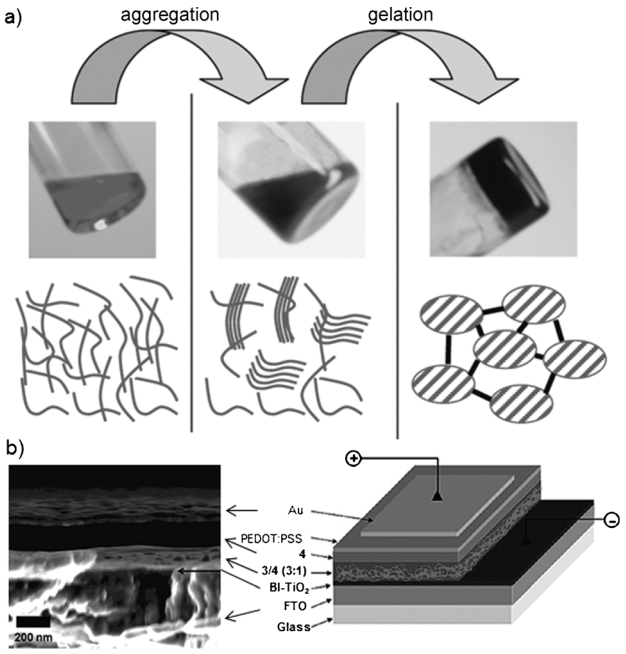

Figure 1. a) Photograph and schematic demonstration of the two-step gelation process of **1** (average-molecular-wieght polymer).[22] b) SEM cross-section and general device architecture of solar cell device fabricated using **3** and **4** with inverted cell configuration.[25] Reproduced with permission from American Chemical Society.

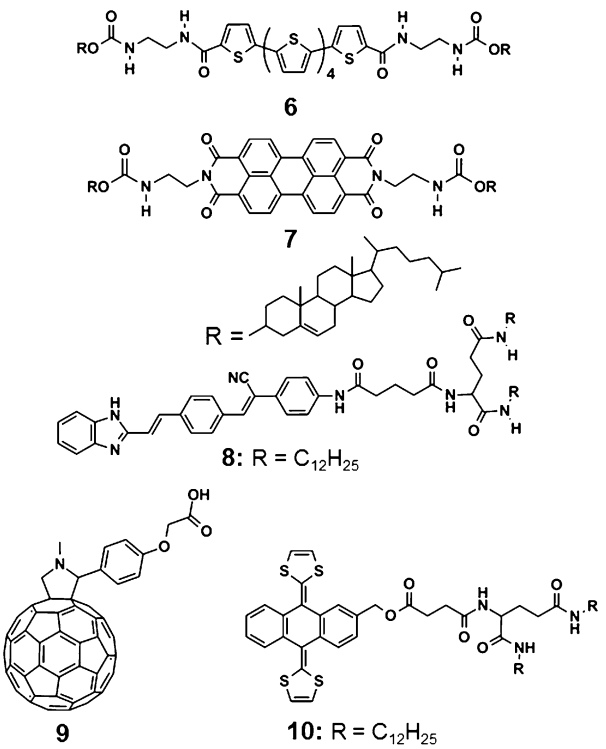

Scheme 2. Chemical structure of compounds **6**–**10**.[27–29]

addition, the photocurrent action spectrum overlaps perfectly with the absorption spectrum, thus indicating that both **6** and **7** act as efficient photoactive species for photocurrent generation (Figure 2b).

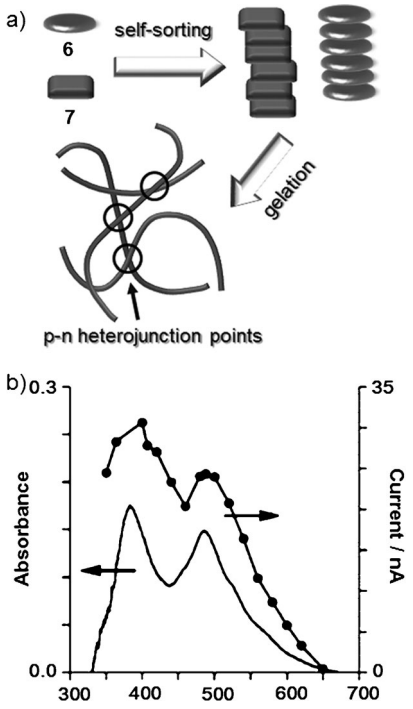

Figure 2. a) Schematic representation of the self-sorting organogel formation of **6** and **7** yielding p-n heterojunction points. b) Absorption spectrum and photocurrent action spectrum of the cast film prepared from **6**/**7** self-sorting gel on an indium tin oxide (ITO) electrode: applied potential = 0.2 V vs. Ag/AgCl.[27] Reproduced with permission from American Chemical Society.

The comparison of changes in emission intensity of the gel of **8** (Scheme 2) upon addition of fullerene (C_{60}) or the C_{60} acid **9** revealed a relatively effective emission quenching by the latter one as a result of stable hydrogen-bonded complex (2:1) formation.[28] Photovoltaic cells fabricated using hybrid gels of **8** and **9** (2:1) as the active layer exhibited steady and large photocurrents relative to those of a device containing **8** and C_{60} in the same ratio. Moreover, the photocurrent increases in proportion to an increase in the positive bias of the ITO electrode. The gelation ability of the tetrathiafulvalene (TTF) derivative **10** (Scheme 2) could be significantly improved by the addition of C_{60} or PCBM because of the intermolecular 2:1 charge-transfer complex formation between the geometrically and electronically complementary ex-TTF (π-extended TTF) and C_{60} units.[29] The photoinduced electron transfer from ex-TTF in **10** to PCBM leads to fast generation of carriers and thereby a steady and rapid, as well as reproducible cathodic photocurrent of 25 nA cm^{-2}. Hence, organogelation is found to be crucial in making good connections, efficient separation between donors and acceptors at the molecular level, and an efficient charge channel along the fibrous direction resulting in an enhanced photocurrent.

A close look at some of the above-mentioned reports reveals that the efficiency of the devices prepared using organogels is not on par with that of devices prepared using polymers. However, organogelators have the advantage of monodispersity of the molecules when compared to the polydispersity and structural defects of polymers. The spontaneous self-assembly of gelators resulting in micrometer-sized large fibers and the presence of a large amount of the insulating alkyl chains may be the reasons for the poor performance. Therefore, it is important to design gelators, the self-assembly of which can be controlled to the level of a few nanometers and thus resulting in nanostructures, with uniform aspect ratios. It is also important to minimize the number of alkyl chains to have closer interaction of molecules. Control of the D–A self-assembly is another crucial issue. Therefore, what is required is the proper addressing of some of these inherent problems as it may help to improve the performance of gelators in the devices.

3. Organogels in OFETs

The recent findings on the better performance of organic nanodevices based on self-assembled structures have encouraged the use of organogelators for OFET applications.[30] OFETs are the key components for electronic tags, flexible circuits, electric paper, sensors, and driving circuits for active matrix displays.[31,32] Since charge carrier mobility is a measure of how easily electrons or holes drift through a semiconductor in response to an electric field, intermolecular ordering plays a crucial role in the design of OFETs.[33,34] Therefore, organization of molecules using a solvent-assisted gelation approach seems to be of great relevance to the design of nanometer-sized architectures useful for the fabrication of OFETs.

Thiophenes and their derivatives are suitable candidates for the fabrication of OFETs because of the improved electronic properties associated with the extended conjugation of oligo- and polythiophenes. However, in many instances the electronic properties of oligomers and polymers can be attained with self-assembled small molecules as a result of strong exciton interaction and electron hopping. The first organogel-based OFET was fabricated by Lee and co-workers using nano/microfibers obtained through organogelation of the dodecyl-substituted thienylvinylene anthracene **11** (Scheme 3).[35] The single-nanofiber transistors (Figure 3a,b) of **11** exhibited p-type characteristics with a hole mobility (μ) of 0.48 cm^2 V^{-1} s^{-1} and a current on/off ratio of 10^5, whereas in the case of a thin film of **11**, a hole mobility within the range of 0.02–0.05 cm^2 V^{-1} s^{-1} was observed. Interestingly, when the FET channel width was reduced to 70 nm, a high mobility value of 8.7 cm^2 V^{-1} s^{-1} was obtained from single-nanofiber transistors.

Comparison to the OFET performance of the semiconducting oligothiophene **12** (Scheme 3) by Stupp and coworkers indicated that self-assembled fibers deposited from a toluene solution exhibit a hole mobility of 3.46×10^{-6} cm^2 V^{-1} s^{-1}, which is one order of magnitude higher than that of films obtained from non-assembling solvents such as

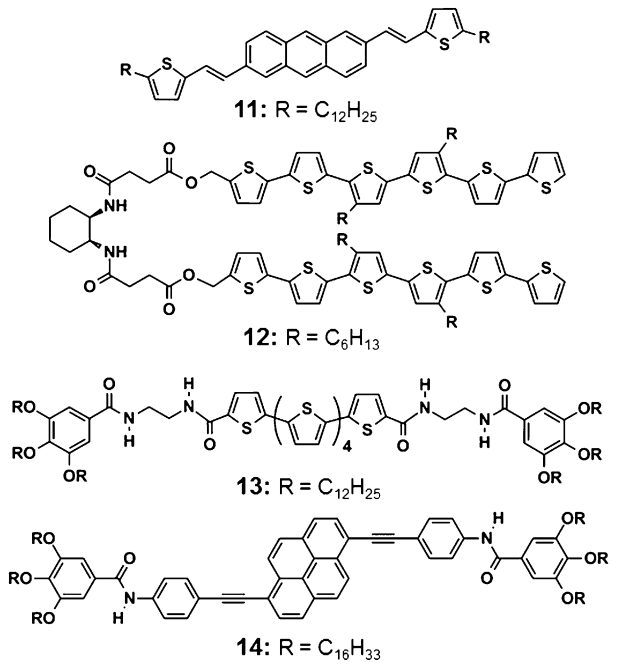

Scheme 3. Chemical structure of compounds **11**–**14**.[35–38]

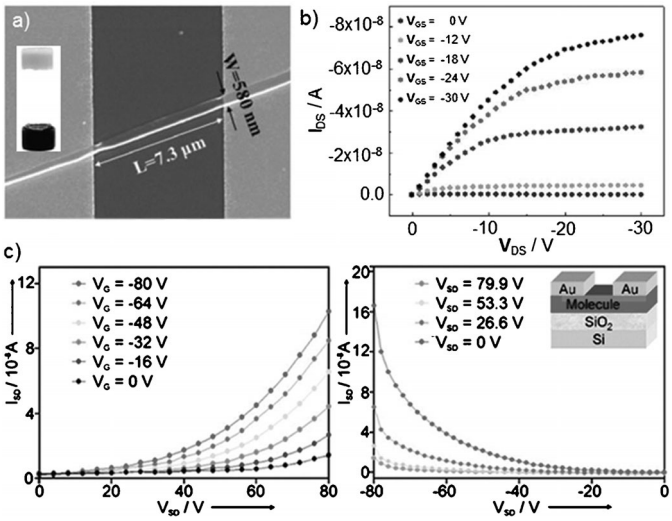

Figure 3. a) SEM image of the bottom-contact single-nanofiber transistor of **11**; inset shows the photograph of the dimethyl sulfoxide gel of **11**.[35] b) Output characteristics of a single-nanofiber transistor of **11**. (Reproduced with permission from Royal Society Chemistry) c) I_{DS}–V_{DS} responses at different gate biases (left) and transduction characteristics (right) for the OFET device fabricated from films of **12** deposited from toluene; inset shows the device configuration of the top-contact OFET.[36] Reproduced with permission from American Chemical Society

chlorobenzene ($9.42\times10^{-7}\,cm^2V^{-1}s^{-1}$) or *o*-chlorobenzene ($1.79\times10^{-7}\,cm^2V^{-1}s^{-1}$; Figure 3c).[36] The self-assembled one-dimensional (1D) nanostructures of the quinquethiophene derivative **13** (Scheme 3) exhibited a hole mobility of $2.34\times10^{-7}\,cm^2V^{-1}s^{-1}$ in a top-contact thin-film transistor device.[37] The gel fibers of the pyrene-substituted 4-ethynylphenylaminoacyl derivative **14** have good electron and hole transport properties as well as light emission in the high source-drain voltage region.[38] The OFET device of the α-helical polypeptide functionalized thiophene gelator **5** and PCBM (1:2; Scheme 1) exhibited an enhanced hole mobility of $1.9\times10^{-7}\,cm^2V^{-1}s^{-1}$ when compared to that of the corresponding nongelaters.[26]

Lutsyk et al. have carried out a comparative study of OFETs fabricated from **1** by spin- and spray-coating techniques using fresh and aged solutions.[39] In all the cases, irrespective of the deposition technique, charge-carrier mobilities in samples fabricated using fresh solutions exhibited values on the order of $10^{-4}\,cm^2V^{-1}s^{-1}$. In contrast, samples fabricated from aged solutions resulted in an increase of the carrier mobilities by one order of magnitude or more, and the highest mobilities exceeded $10^{-2}\,cm^2V^{-1}s^{-1}$. This observation indicates that anisotropy resulting from the ordering of nanofibers and gelation upon ageing has a significant influence on the carrier mobility. In the above cases, the high mobility values obtained for assemblies generated from the gelling solvents is attributed to the better organization of the semiconducting gelator molecules into self-assembled 1D nanostructures having strong π-orbital overlap, which improves the hole mobility and thereby generates better charge transport pathways.

Notably, as in the case of OSCs, publications related to the use of organogels in OFETs are very few when compared to the use of polymers and small molecules. Even though the electronic properties of molecular self-assemblies and gels are comparable to polymers in many cases, the device performances achieved so far are relatively poor. As discussed earlier, the spontaneous self-assembly leading to fast growth of fibers, the presence of a large number of aliphatic side chains, and the amorphous nature of the self-assemblies may be some of the reasons for the poor performances. It is also challenging to achieve macroscopic alignment of the self-assemblies for better performance. Irrespective of the above inherent problems, encouraging results pertaining to improved electronic properties of self-assemblies and gels are appearing. Therefore, the organogelation route will continue to motivate researchers to develop low-cost, flexible organic transistors.

4. Conductive Organogels

After discussing the recent developments pertaining to the use of organogels in OSCs and OFETs we now highlight the recent developments with conducting materials based on the self-assembly of functional π-conjugated molecules. Preparation of such soft materials are important to the design of energy efficient devices.[40] In this context, the improvement of conductivity through intermolecular interactions of the closely assembled gelator molecules in the gel state is significant, thus providing a bulk conducting nanowire.[40–42] Even though such supramolecular wires offer many advantages, controlling the self-assembly process during gelation is a challenging task. Therefore, in many cases, conducting properties were investigated for both the film state and nanostructures formed from solutions of different substrates.[43–48]

As mentioned earlier thiophenes are one of the most widely used organic heterocyclic building blocks for the preparation of conducting materials because of its synthetic accessibility, unique optoelectronics, redox and charge transport properties.[49] Stupp and co-workers have used the advantage of characteristic microphase segregation of diblock polymers during self-assembly to design electronically active and functional supramolecular architectures of the oligo(thiophene) dendron rod-coil (DRC) molecule **15** (Scheme 4).[50] The improved π-orbital overlap along conductive pathways in the iodine-doped films of **15** from a toluene gel exhibited conductivity that was three orders of magnitude higher ($7.9\times10^{-5}\,S\,cm^{-1}$) than that from the monomer solution ($8.0\times10^{-8}\,S\,cm^{-1}$). The amide-end-functionalized trithienylenevinylene (TTV) molecular gelators (**16** and **17**) are reported to show high charge-carrier properties in the self-assembled state in the presence of *N*,*N*′-bis(2,5-di-*tert*-butylphenyl)-3,4,9,10-perylenedicarboximide (PDI).[51] Unlike other π gelators that form entangled fibrous structures on a mica surface, AFM images of **16** and **17** from *n*-decane exhibited oriented 1D fibers for **16** and interconnected short wires with T junctions for **17** (Figures 4 a,b).

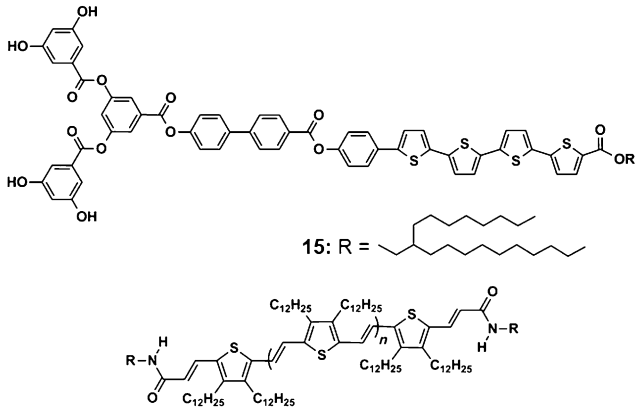

Scheme 4. Chemical structure of compounds **15**–**19**.[50–52]

The flash photolysis time-resolved microwave transient conductivity (FP-TRMC) profiles of the drop casted films from chloroform showed charge-carrier mobility values, $\Sigma\mu_{min}$, of $1.5\times10^{-2}\,cm^2V^{-1}s^{-1}$ and $4.0\times10^{-2}\,cm^2V^{-1}s^{-1}$, whereas xerogels prepared from an *n*-decane/chloroform mixture (1:1) exhibited $\Sigma\mu_{min}$ values of $6.0\times10^{-2}\,cm^2V^{-1}s^{-1}$ and $7.4\times10^{-2}\,cm^2V^{-1}s^{-1}$ respectively for the TTV compounds **16** and **17** (Figures 5 a,b). Organogels with high conductivity were obtained by extending the conjugation length of the oligo(thienylenevinylene) gelator (**18** and **19**).[52] The conductive atomic force microscopy (C-AFM) measurements indicated a conductance of 0.93 nS for the undoped fiber bundles of **19**, and the conductance drastically increased to 7.1 nS upon doping with iodine vapors (Figures 5 c,d). In addition, the room temperature bulk electrical conductivities (σ) of the undoped films of **18** and **19**, measured using four-probe method, exhibited values of 6.4×10^{-4} and $4.9\times10^{-2}\,S\,cm^{-1}$, respectively. After doping with iodine vapors, these values showed enhancements of two orders of magnitude, thus increasing to 1.0×10^{-2} and $4.8\,S\,cm^{-1}$, respectively.

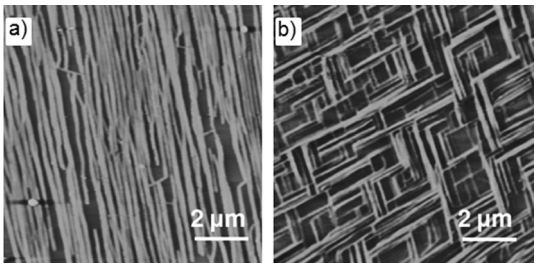

Figure 4. AFM images of a) **16** and b) **17** drop casted from *n*-decane on freshly cleaved mica (5×10^{-5} M). The *Z* scales used in a) are 40 nm and in b) are 20 nm.[51] Reproduced with permission from American Chemical Society.

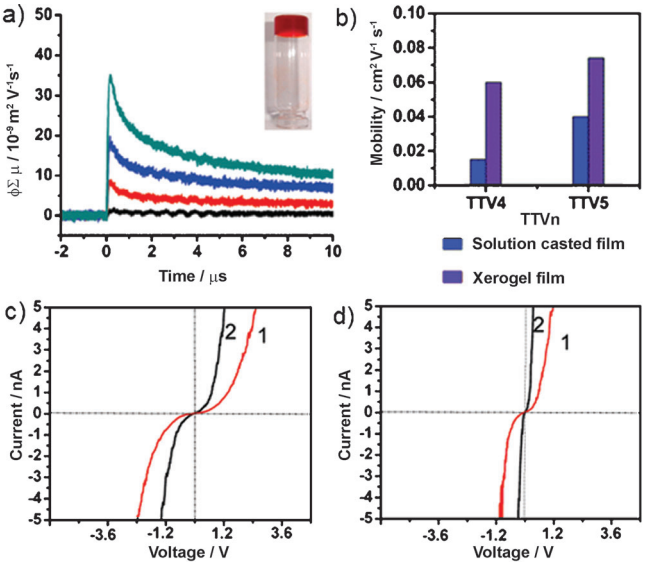

Figure 5. a) FP-TRMC transient conductivity profiles ($\lambda_{ex}=355$ nm) of **17** with PDI films prepared from *n*-decane/chloroform (1:1 v/v) solutions. The color represents weight fraction of PDI relative to 100 wt% **17**. The value of ϕ (quantum efficiency of charge carrier generation) at the peak of each PDI fraction was estimated by TAS (transient absorption spectra), giving 0.39–0.99% for 0.23–1.2%; inset shows the photograph of the *n*-decane gel of **17**. b) Comparison of the charge-carrier mobility values of **16** and **17** from solution-cast films and xerogels.[51] c,d) C-AFM measurements of **18** and **19** xerogels from an *n*-decane solution drop casted on HOPG (highly ordered pyrolytic graphite. *I*–*V* curves of undoped (c) and doped (d) xerogels of **18** (1) and **19** (2).[52] Reproduced with permission from American Chemical Society.

The barbituric acid functionalized quaterthiophene **20** (Scheme 5) forms conductive gels through complementary hydrogen bonds with a flexible bis(melamine) receptor.[53] The irradiation using a laser pulse ($\lambda=355$ nm) resulted in the generation of long-lived charge carriers with maximum transient conductivities ($\phi\Sigma\mu$) of $1.0\times10^{-4}\,cm^2V^{-1}s^{-1}$ for **20** and $0.67\times10^{-4}\,cm^2V^{-1}s^{-1}$ for the coassembly (Figure 6).

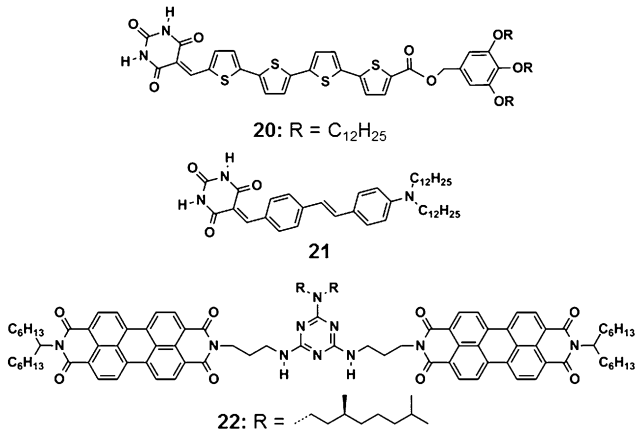

Scheme 5. Chemical structure of compounds **20**–**22**.[53–55]

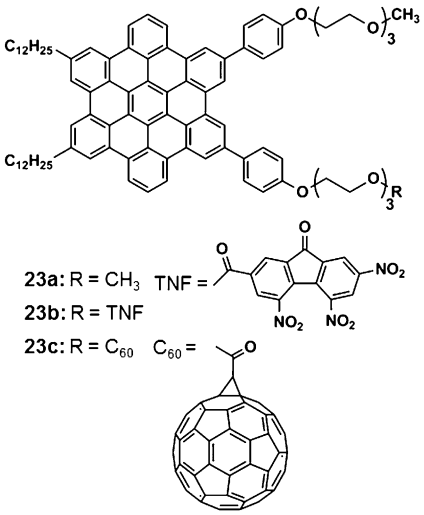

Scheme 6. Chemical structure of compounds **23a**–**c**.[56–60]

Even though, interchain transportation of charge carriers within the lamella decreased the hole mobility (μ^+) of coassembled tapes to 0.57 $cm^2V^{-1}s^{-1}$, 1D hole mobility along the long axis of nanorods (μ^+_{1D}) exhibited the higher value of 1.3 $cm^2V^{-1}s^{-1}$.

The nematic gel-forming supramolecular complex of **21** (Scheme 5) and the complementary hydrogen-bonding unit, comprised of ribbon-like aggregates exhibited a higher $\phi\Sigma\mu$ value of 5.2×10^{-6} $cm^2V^{-1}s^{-1}$ than the vesicular aggregates of **21** (4.4×10^{-6} $cm^2V^{-1}s^{-1}$).[54] Also a higher 1D isotropic mobility ($\phi\mu = 5.1\times10^{-3}$ $cm^2V^{-1}s^{-1}$) of the photogenerated charge carriers was observed for the binary system. The chiral discotic supramolecular complexes of monotopically triple-hydrogen-bonding melamines equipped with two perylene bisimide (PBI) chromophores with tritopically triple-hydrogen-bonding cyanuric acid **22** showed a reproducible $\phi\Sigma\mu$ value of 1.4×10^{-5} $cm^2V^{-1}s^{-1}$ and $\phi\mu$ of 0.03 $cm^2V^{-1}s^{-1}$.[55]

Fused polyaromatic systems are ideal candidates for the creation of a 1D discotic structure with high charge-carrier mobility. For example, the self-assembly of the amphiphilic hexabenzocoronene (HBC) **23a** (Scheme 6) bearing two dodecyl chains (C_{12}) on one side and two triethylene glycol (TEG) chains on the other forms redox active, electroconductive nanotubes and gels.[56,57] The electrical resistivity of the nanotubes was found to be 2.5 MΩ upon oxidation with nitrosonium tetrafluoroborate ($NOBF_4$).[56] In another report, nanotubes of the trinitrofluoronene-substituted HBC amphiphile **23b** exhibited a photocurrent of 4.2 nA and a dark current of 0.07 pA.[58] Significant enhancement in photoconductivity has been achieved by varying the amount of **23b** in nanotubes of **23a** (Figure 7b), thus indicating a bell-shaped dependency on the mole fraction of **23b** (Figure 7b).[59] The rapid excitation energy migration along the π-stacked HBC layers enabled efficient electron transfer, and thereby charge separation (Figure 7c). In the case of amphiphilic HBC **23c** having an appended C_{60}, the field-effect charge-carrier mobility measurements revealed an ambipolar charge-carrier hole mobility (μ_h) of 9.7×10^{-7} $cm^2V^{-1}s^{-1}$ and electron mobility (μ_e) of 1.1×10^{-5} $cm^2V^{-1}s^{-1}$.[60]

The peculiar coaxial configuration of the nanotubes with a π-stacked HBC array covered by a molecular layer of C_{60} facilitates a photovoltaic response upon illumination with light. Interestingly, the nanotube of **23a** exhibited a p-type FET property with a μ_h value of 1.0×10^{-4} $cm^2V^{-1}s^{-1}$, which is two orders of magnitude greater than that observed for the homotropic nanotube of **23c**. The coassembly of **23a** and **23c** strongly reflects the ambipolar carrier transport properties, which enhances the performance of the system by balancing the hole and electron transporting components. FP-TRMC

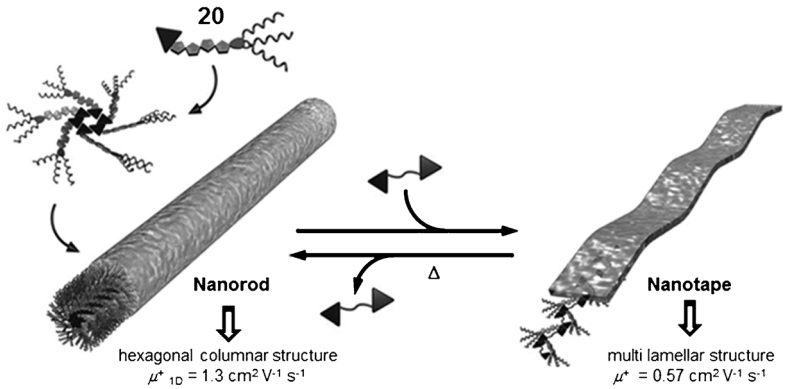

Figure 6. Schematic representation of interconversion between nanorods and nanotapes of **20**.[53] Reproduced with permission from Wiley-VCH.

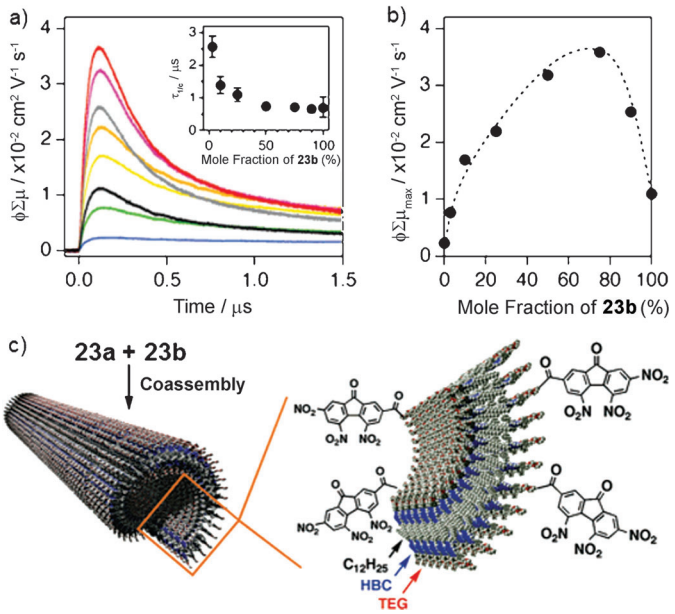

Figure 7. a) FP-TRMC profiles of cast films of the nanotubes with varying mole fractions of **23b**: 0 (blue), 3 (green), 10 (yellow), 25 (orange), 50 (pink), 75 (red), 90 (grey), and 100% (black), upon photoirradiation at 355 nm (photon density, 1.2×10^{15} cm^{-2}). Inset shows the plot of $\tau_{1/e}$ values versus mole fractions of **23b**. b) Plot of $\phi\Sigma\mu_{max}$ values versus mole fractions of **23b**. c) Schematic illustration of the coassembled nanotube from **23a** and **23b**.[59] Reproduced with permission from American Chemical Society.

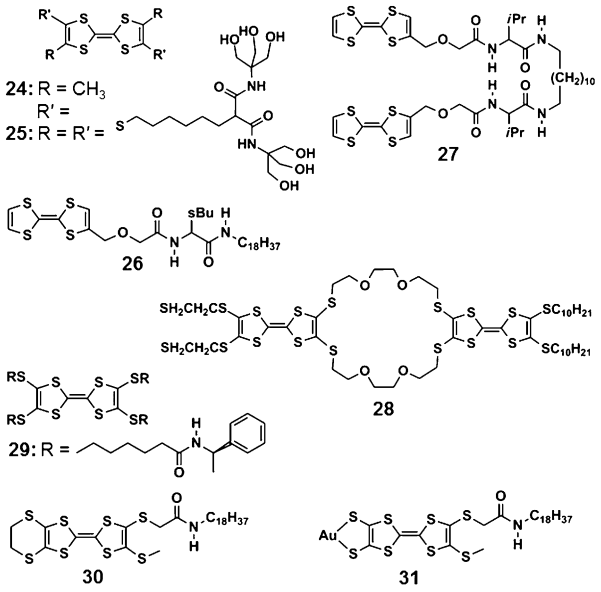

Scheme 7. Chemical structure of compounds **24**–**31**.[66–72]

measurements of the coassembled nanotubes exhibited a carrier mobility of 1.4–2.0 cm^{2}V^{-1}s^{-1}, which is close to the intersheet mobility in graphite.

TTF is one among the most extensively studied sulfur-containing conductive materials which exhibits high electron conductivity because of π-stacked columnar structures.[61–65] The self-assembled molecular wires of a TTF gel (**24**, Scheme 7) was introduced in 1994 by Jørgensen and co-workers.[66] Bryce et al. have reported the first experimental demonstration of a conductive TTF gel using spin-coated films of **25**.[67] The ohmic current/voltage measurements of the spin-coated films of **25** exhibited an in-plane direct current (dc) conductivity value (σ_{rt}) of 10^{-6} S cm^{-1}, which was additionally increased to 10^{-4} S cm^{-1} for iodine-doped films and 10^{-5}–10^{-4} S cm^{-1} for tetrabutylammonium-perchlorate- or hexafluorophosphate-doped films. Conducting gel-liquid crystal composites (**26**, **27**) are shown to have insulator character (**26**: $\sigma_{rt} < 3\times10^{-10}$ S cm^{-1}), however, the conductivity significantly increased after exposure to I_2 for 2 minutes ($\sigma_{rt} = 2\times10^{-7}$ S cm^{-1}).[68] Interestingly, the conductivity value additionally improved to 1×10^{-5} S cm^{-1} after doping with tetracyanoquinodimethane (TCNQ).

An amphiphilic bis-TTF annulated macrocyclic derivative **28** (Scheme 7) reported by Nakamura et al. formed redox active organogels as well as electrically active nanostructures such as size-controllable nanodots and nanowires (Figure 8a,b).[69] The observed conductance of 20 nS for a single nanodot formed by the chemically oxidized **28** has been increased to 86 nS under ambient conditions as a result of the effects of oxygen and/or water. The conductance of a single nanodot with an open-shell electronic structure was four to five orders of magnitude higher than that of fibers with a closed-shell electronic structure and fiber bundles (Figures 8a–c). In the case of 1D charge-transfer (CT) assemblies of oxidized TTFs and other electron acceptors, high electronic conductivity is strongly dependent upon the magnitude of intermolecular CT interactions and the length of the stacks.[70] In this context, a combination of intermolecular hydrogen bonding and charge-transfer complex formation has been used for making stable conductive TTF nanofibers of **29**. In the presence of a stoichiometric amount of the electron acceptor 2,3,5,6-tetrafluoro-7,7,8,8-tetracyanoquinodimethane (F4TCNQ), **29** yielded a dark-colored CT gel with electrical conductivity of 5.0×10^{-4} S cm^{-1}. In addition, the electrical conductivity of individual nanofibers measured using point-contact current-imaging atomic force microscopy (PCI-AFM) estimated a one-dimensional resistivity of $7.0\pm3.0\times10^{-4}$ S cm^{-1} of a single nanofiber.

In recent years a variety of TTF-based conducting gels have been reported because of their excellent redox active properties.[71–80] In contrast to other TTF gels, the amide-functionalized TTF derivative **30** (Scheme 7), reported by Amabilino et al., exhibited interesting electronic properties.[71] The four-probe dc resistance measurements of the doped xerogel of **30** exhibited conductivity (σ) of 3–5 × 10^{-3} Ω^{-1}cm^{-1}. The room temperature resistivity of the irreversible thermally converted β phase (semiconducting) of the doped xerogel was found to be one order less than that of the α phase. Interestingly, in the bright areas of the xerogel, *I*–*V* response exhibited an apparent metallic character, whereas in dark areas a semiconductor character with a wide gap was observed (Figure 8d). A hybrid gel of **31** and **30** enabled incorporation of gold nanoparticles within the TTF gel fibers, which self-organized into a secondary structure with metallic conductivity.[72] Room temperature *I*–*V* sweeps of the doped hybrid nanofibers exhibited better metallic

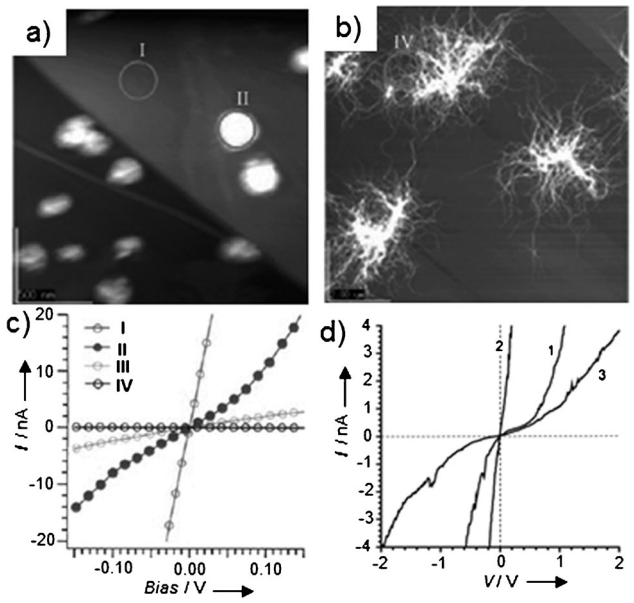

Figure 8. AFM images of a) nanodots of **28**/$(I_2)_2$ and b) fibrous structures of **28** on HOPG (10×10 mm^2) prepared by spin casting of a 1 mM solution ($CHCl_3/CH_3CN$ 6:4). c) *I–V* characteristics at points I (HOPG), II (single nanodot in air), III (single nanodot in vacuum at 5×10^{-3} Pa), and IV (bundle of fibers).[68] d) Current-sensing AFM spectroscopic curves of different areas of the xerogel of **30** on graphite.[71] Reproduced with permission from Wiley-VCH.

behavior with a conductivity of 10 S cm^{-1} whereas **31** showed five times less conductivity when doped. The advantage of the hybrid system is that the mixed-valent donor stacks attain a highly conducting β phase without any heat treatment, immediately after doping. Even though detailed understanding of the electronic properties of conducting gels have been achieved, application of these functional supramolecular nanostructures needs more attention for their successful incorporation into electronic devices.

5. Conclusions and Perspectives

In this Minireview we have discussed the pros and cons of the gelation approach to create functional assemblies of electronically active π-conjugated materials for device applications. The simplicity of the gelation approach and tunability of the properties of gelator molecules have contributed significantly towards the development of π-gelator-based electronic devices. Since BHJ OSCs show better charge separation efficiency, design of donor–acceptor-based supramolecular gels with nanowire morphology is important. The challenge is to achieve self-sorted 1D assemblies of the donors and the acceptors resulting in longitudinal BHJs with optimal charge separation. These goals can be achieved only through the logical design of new molecules and their conversion into stable, shape- and size-controlled 1D supramolecular structures. In the context of gathering momentum for the development of efficient OSCs, gel chemistry is expected to play a crucial role in the design of low-cost and flexible BHJ photovoltaic devices with high performance. Even though organogel nanostructures have been employed in different applications, the end use as an integral part of organic electronic devices remains to be proven in terms of the efficiency and longevity of the device. The coming years are expected to witness a myriad of activities to address the need for the future energy requirements. Therefore, we hope that intense research on the use of organic materials, whether it be polymers, small molecules, or gels, needs to be continued to achieve the dream of large-area organic photovoltaic devices with high light conversion efficiency; such devices are the ultimate source of sustainable green energy for future needs. The inspiration for young researchers to work in the area of self-assembly and gel-based materials derives from the fact that a breakthrough is yet to come.

A.A. is grateful to the Department of Atomic Energy, Government of India for a DAE-SRC Outstanding Researcher Award and CSIR, Government of India for partial financial support under NWP-23 (Manuscript no. PPG-321 from NIIST). CSIR, Government of India, is acknowledged for a research fellowship to S.P.

Received: September 23, 2011
Published online: January 25, 2012

[1] F. J. M. Hoeben, P. Jonkheijm, E. W. Meijer, A. P. H. J. Schenning, *Chem. Rev.* **2005**, *105*, 1491 – 1546.
[2] J.-M. Lehn, *Science* **2002**, *295*, 2400 – 2403.
[3] P. Terech, R. G. Weiss, *Chem. Rev.* **1997**, *97*, 3133 – 3159.
[4] D. J. Abdallah, R. G. Weiss, *Adv. Mater.* **2000**, *12*, 1237 – 1247.
[5] A. Ajayaghosh, V. K. Praveen, C. Vijayakumar, *Chem. Soc. Rev.* **2008**, *37*, 109 – 122.
[6] A. Ajayaghosh, V. K. Praveen, *Acc. Chem. Res.* **2007**, *40*, 644 – 656.
[7] A. Dawn, T. Shiraki, S. Haraguchi, S.-i. Tamaru, S. Shinkai, *Chem. Asian J.* **2010**, *5*, 266 – 282.
[8] T. Kato, Y. Hirai, S. Nakaso, M. Moriyama, *Chem. Soc. Rev.* **2007**, *36*, 1857 – 1867.
[9] *Hybrid Materials, Synthesis, Characterization and Applications* (Ed.: G. Kickelbick), Wiley-VCH, Weinheim, Germany, **2007**.
[10] G. O. Lloyd, J. W. Steed, *Nat. Chem.* **2009**, *1*, 437 – 442.
[11] A. R. Hirst, B. Escuder, J. F. Miravet, D. K. Smith, *Angew. Chem.* **2008**, *120*, 8122 – 8139; *Angew. Chem. Int. Ed.* **2008**, *47*, 8002 – 8018.
[12] J. Roncali, *Acc. Chem. Res.* **2009**, *42*, 1719 – 1730.
[13] A. W. Hains, Z. Liang, M. A. Woodhouse, B. A. Gregg, *Chem. Rev.* **2010**, *110*, 6689 – 6735.
[14] S.-S. Sun, N. S. Sariciftci, *Organic Photovoltaics: Mechanisms, Materials and Devices*, Taylor and Francis, Boca Raton, **2005**.
[15] P. Heremans, D. Cheyns, B. P. Rand, *Acc. Chem. Res.* **2009**, *42*, 1740 – 1747.
[16] W. Kubo, K. Murakoshi, T. Kitamura, S. Yoshida, M. Haruki, K. Hanabusa, H. Shirai, Y. Wada, S. Yanagida, *J. Phys. Chem. B* **2001**, *105*, 12809 – 12815.
[17] W. Kubo, T. Kitamura, K. Hanabusa, Y. Wada, S. Yanagida, *Chem. Commun.* **2002**, 374 – 375.
[18] N. Mohmeyer, P. Wang, H.-W. Schmidt, S. M. Zakeeruddin, M. Grätzel, *J. Mater. Chem.* **2004**, *14*, 1905 – 1909.
[19] G. Li, V. Shrotriya, J. Huang, Y. Yao, T. Moriarty, K. Emery, Y. Yang, *Nat. Mater.* **2005**, *4*, 864 – 868.
[20] F. Padinger, R. S. Rittberger, N. S. Sariciftci, *Adv. Funct. Mater.* **2003**, *13*, 85 – 88.

[21] W. Y. Huang, P. T. Huang, Y. K. Han, C. C. Lee, T. L. Hsieh, M. Y. Chang, *Macromolecules* **2008**, *41*, 7485 – 7489.
[22] M. Koppe, C. J. Brabec, S. Heiml, A. Schausberger, W. Duffy, M. Heeney, I. McCulloch, *Macromolecules* **2009**, *42*, 4661 – 4666.
[23] B.-G. Kim, E. J. Jeong, H. J. Park, D. Bilby, L. J. Guo, J. Kim, *ACS Appl. Mater. Interfaces* **2011**, *3*, 674 – 680.
[24] J. J. Richards, K. M. Weigandt, D. C. Pozzo, *J. Colloid Interface Sci.* **2011**, *364*, 341 – 350.
[25] A. Wicklein, S. Ghosh, M. Sommer, F. Würthner, M. Thelakkat, *ACS Nano* **2009**, *3*, 1107 – 1114.
[26] R. J. Kumar, J. M. MacDonald, T. B. Singh, L. J. Waddington, A. B. Holmes, *J. Am. Chem. Soc.* **2011**, *133*, 8564 – 8573.
[27] K. Sugiyasu, S.-i. Kawano, N. Fujita, S. Shinkai, *Chem. Mater.* **2008**, *20*, 2863 – 2865.
[28] P. Xue, R. Lu, L. Zhao, D. Xu, X. Zhang, K. Li, Z. Song, X. Yang, M. Takafuji, H. Ihara, *Langmuir* **2010**, *26*, 6669 – 6675.
[29] X. Yang, G. Zhang, D. Zhang, D. Zhu, *Langmuir* **2010**, *26*, 11720 – 11725.
[30] V. Coropceanu, J. Cornil, D. A. D. S. Filho, Y. Olivier, R. J. Silbey, J. L. Brédas, *Chem. Rev.* **2007**, *107*, 926 – 952.
[31] A. Tsumura, K. Koezuka, T. Ando, *Appl. Phys. Lett.* **1986**, *49*, 1210.
[32] H. Klauk, *Organic Electronics: Materials, Manufacturing and Applications*, Wiley-VCH, Weinheim, **2006**.
[33] J. Smith, R. Hamilton, I. McCulloch, N. Stingelin-Stutzmann, M. Heeney, D. D. C. Bradley, T. D. Anthopoulos, *J. Mater. Chem.* **2010**, *20*, 2562 – 2574.
[34] M. Mas-Torrent, C. Rovira, *Chem. Soc. Rev.* **2008**, *37*, 827 – 838.
[35] J.-P. Hong, M.-C. Um, S.-R. Nam, J.-I. Hong, S. Lee, *Chem. Commun.* **2009**, 310 – 312.
[36] W.-W. Tsai, I. D. Tevis, A. S. Tayi, H. Cui, S. I. Stupp, *J. Phys. Chem. B* **2010**, *114*, 14778 – 14786.
[37] D. A. Stone, A. S. Tayi, J. E. Goldberger, L. C. Palmera, S. I. Stupp, *Chem. Commun.* **2011**, *47*, 5702 – 5704.
[38] S. Diring, F. Camerel, B. Donnio, T. Dintzer, S. Toffanin, R. Capelli, M. Muccini, R. Ziessel, *J. Am. Chem. Soc.* **2009**, *131*, 18177 – 18185.
[39] U. Bielecka, P. Lutsyk, K. Janus, J. Sworakowski, W. Bartkowiak, *Org. Electron.* **2011**, *12*, 1768 – 1776.
[40] M. Hasegawa, M. Iyoda, *Chem. Soc. Rev.* **2010**, *39*, 2420 – 2427.
[41] M. Iyoda, M. Hasegawa, H. Enozawa, *Chem. Lett.* **2007**, *36*, 1402 – 1407.
[42] F. S. Schoonbeek, J. H. van Esch, B. Wegewijs, D. B. A. Rep, M. P. de Haas, T. M. Klapwijk, R. M. Kellogg, B. L. Feringa, *Angew. Chem.* **1999**, *111*, 1486 – 1490; *Angew. Chem. Int. Ed.* **1999**, *38*, 1393 – 1397.
[43] N. Kiriy, V. Bocharova, A. Kiriy, M. Stamm, F. C. Krebs, H.-J. Adler, *Chem. Mater.* **2004**, *16*, 4765 – 4771.
[44] X.-Q. Li, V. Stepanenko, Z. Chen, P. Prins, L. D. A. Siebbeles, F. Würthner, *Chem. Commun.* **2006**, 3871 – 3873.
[45] O. J. Dautel, M. Robitzer, J.-C. Flores, D. Tondelier, F. Å. Serein-Spirau, J.-P. Lére-Porte, D. Guérin, S. Lenfant, M. Tillard, D. Vuillaume, J. J. E. Moreau, *Chem. Eur. J.* **2008**, *14*, 4201 – 4213.
[46] J. W. Chung, H. Yang, B. Singh, H. Moon, B.-k. An, S. Y. Lee, S. Y. Park, *J. Mater. Chem.* **2009**, *19*, 5920 – 5925.
[47] P. Pratihar, S. Ghosh, V. Stepanenko, S. Patwardhan, F. C. Grozema, L. D. A. Siebbeles, F. Würthner, *Beilstein J. Org. Chem.* **2010**, *6*, 1070 – 1078.
[48] S. Yagai, T. Seki, H. Murayama, Y. Wakikawa, T. Ikoma, Y. Kikkawa, T. Karatsu, A. Kitamura, Y. Honsho, S. Seki, *Small* **2010**, *6*, 2731 – 2740.
[49] A. Mishra, C.-Q. Ma, P. Bäuerle, *Chem. Rev.* **2009**, *109*, 1141 – 1276.
[50] J. F. Hulvat, M. Sofos, K. Tajima, S. I. Stupp, *J. Am. Chem. Soc.* **2005**, *127*, 366 – 372.
[51] S. Prasanthkumar, A. Saeki, S. Seki, A. Ajayaghosh, *J. Am. Chem. Soc.* **2010**, *132*, 8866 – 8867.
[52] S. Prasanthkumar, A. Gopal, A. Ajayaghosh, *J. Am. Chem. Soc.* **2010**, *132*, 13206 – 13207.
[53] S. Yagai, T. Kinoshita, Y. Kikkawa, T. Karatsu, A. Kitamura, Y. Honsho, S. Seki, *Chem. Eur. J.* **2009**, *15*, 9320 – 9324.
[54] S. Yagai, Y. Nakano, S. Seki, A. Asano, T. Okubo, T. Isoshima, T. Karatsu, A. Kitamura, Y. Kikkawa, *Angew. Chem.* **2010**, *122*, 10186 – 10190; *Angew. Chem. Int. Ed.* **2010**, *49*, 9990 – 9994.
[55] T. Seki, A. Asano, S. Seki, Y. Kikkawa, H. Murayama, T. Karatsu, A. Kitamura, S. Yagai, *Chem. Eur. J.* **2011**, *17*, 3598 – 3608.
[56] J. P. Hill, W. Jin, A. Kosaka, T. Fukushima, H. Ichihara, T. Shimomura, K. Ito, T. Hashizume, N. Ishii, T. Aida, *Science* **2004**, *304*, 1481 – 1483.
[57] Y. Yamamoto, G. Zhang, W. Jin, T. Fukushima, N. Ishii, A. Saeki, S. Seki, S. Tagawa, T. Minari, K. Tsukaghosi, T. Aida, *Proc. Natl. Acad. Sci. USA* **2005**, *102*, 10801 – 10806.
[58] Y. Yamamoto, T. Fukushima, Y. Suna, N. Ishii, A. Saeki, S. Seki, S. Tagawa, M. Taniguchi, T. Kawai, T. Aida, *Science* **2006**, *314*, 1761 – 1764.
[59] Y. Yamamoto, T. Fukushima, A. Saeki, S. Seki, S. Tagawa, N. Ishii, T. Aida, *J. Am. Chem. Soc.* **2007**, *129*, 9276 – 9277.
[60] Y. Yamamotoa, G. Zhanga, W. Jina, T. Fukushima, N. Ishii, A. Saeki, S. Seki, S. Tagawa, T. Minari, K. Tsukagoshi, T. Aida, *Proc. Natl. Acad. Sci. USA* **2009**, *106*, 21051 – 21056.
[61] D. B. Amabilino, J. Puigmartí-Luis, *Soft Matter* **2010**, *6*, 1605 – 1612.
[62] Y.-L. Zhao, I. Aprahamian, A. Trabolsi, N. Erina, J. F. Stoddart, *J. Am. Chem. Soc.* **2008**, *130*, 6348 – 6350.
[63] H. Enozawa, Y. Honna, M. Iyoda, *Chem. Lett.* **2007**, *36*, 1434 – 1435.
[64] C. Wang, D. Zhang, D. Zhu, *J. Am. Chem. Soc.* **2005**, *127*, 16372 – 16373.
[65] J. Sly, P. Kasák, E. Gomar-Nadal, C. Rovira, L. Górriz, P. Thordarson, D. B. Amabilino, A. E. Rowan, R. J. M. Nolte, *Chem. Commun.* **2005**, 1255 – 1257.
[66] M. Joergensen, K. Bechgaard, T. Bjoernholm, P. Sommer-Larsen, L. G. Hansen, K. Schaumburg, *J. Org. Chem.* **1994**, *59*, 5877 – 5882.
[67] T. L. Gall, C. Pearson, M. R. Bryce, M. C. Petty, H. Dahlgaard, J. Becher, *Eur. J. Org. Chem.* **2003**, 3562 – 3568.
[68] T. Kitamura, S. Nakaso, N. Mizoshita, Y. Tochigi, T. Shimomura, M. Moriyama, K. Ito, T. Kato, *J. Am. Chem. Soc.* **2005**, *127*, 14769 – 14775.
[69] T. Akutagawa, K. Kakiuchi, T. Hasegawa, S.-i. Noro, T. Nakamura, H. Hasegawa, S. Mashiko, J. Becher, *Angew. Chem.* **2005**, *117*, 7449 – 7453; *Angew. Chem. Int. Ed.* **2005**, *44*, 7283 – 7287.
[70] Y. Tatewaki, T. Hatanaka, R. Tsunashima, T. Nakamura, M. Kimura, H. Shirai, *Chem. Asian J.* **2009**, *4*, 1474 – 1479.
[71] J. Puigmartí-Luis, V. Laukhin, Á. P. del Pino, J. Vidal-Gancedo, C. Rovira, D. B. Amabilino, *Angew. Chem.* **2007**, *119*, 242 – 245; *Angew. Chem. Int. Ed.* **2007**, *46*, 238 – 241.
[72] J. Puigmartí-Luis, Á. P. del Pino, E. Laukhina, J. Esquena, V. Laukhin, C. Rovira, J. Vidal-Gancedo, A. G. Kanaras, R. J. Nichols, M. Brust, D. B. Amabilino, *Angew. Chem.* **2008**, *120*, 1887 – 1891; *Angew. Chem. Int. Ed.* **2008**, *47*, 1861 – 1865.
[73] I. Danila, F. Riobé, J. Puigmartí-Luis, Á. P. del Pino, J. D. Wallis, D. B. Amabilino, N. Avarvari, *J. Mater. Chem.* **2009**, *19*, 4495 – 4504.
[74] J. Puigmartí-Luis, Á. P. del Pino, V. Laukhin, L. N. Feldborg, C. Rovira, E. Laukhina, D. B. Amabilino, *J. Mater. Chem.* **2010**, *20*, 466 – 474.
[75] E. Torres, J. Puigmartí-Luis, Á. P. del Pino, R. M. Ortuño, D. B. Amabilino, *Org. Biomol. Chem.* **2010**, *8*, 1661 – 1665.
[76] D. Caneveta, Á. P. del Pino, D. B. Amabilino, M. Sallé, *J. Mater. Chem.* **2011**, *21*, 1428 – 1437.

[77] E. Taboada, L. N. Feldborg, A. P. del Pino, A. Roig, D. B. Amabilino, J. Puigmartí-Luis, *Soft Matter* **2011**, *7*, 2755 – 2761.
[78] S. Ahn, Y. Kim, S. Beak, S. Ishimoto, H. Enozawa, E. Isomura, M. Hasegawa, M. Iyoda, Y. Park, *J. Mater. Chem.* **2010**, *20*, 10817 – 10823.
[79] X.-J. Wang, L.-B. Xing, W.-N. Cao, X.-B. Li, B. Chen, C.-H. Tung, L.-Z. Wu, *Langmuir* **2011**, *27*, 774 – 781.
[80] C. Wang, Q. Chen, F. Sun, D. Zhang, G. Zhang, Y. Huang, R. Zhao, D. Zhu, *J. Am. Chem. Soc.* **2010**, *132*, 3092 – 3096.